Journal of Solid State Chemistry 182 (2009) 3217–3221

Contents lists available at ScienceDirect

Journal of Solid State Chemistry

journal homepage: www.elsevier.com/locate/jssc

Investigation of structural and magnetic properties of nanocrystalline manganese substituted lithium ferrites

P.P. Hankare [a,*], R.P. Patil [a], U.B. Sankpal [a], S.D. Jadhav [a], P.D. Lokhande [b], K.M. Jadhav [c], R. Sasikala [d]

[a] Department of Chemistry, Shivaji University, Kolhapur 416004, Maharashtra, India
[b] Pune University, Pune, Maharashtra, India.
[c] Dr. B.A.Marathwada University, Aurangabad 431004, Maharashtra, India
[d] Chemistry Division, Bhabha Atomic Research Center, Mumbai 400085, Maharashtra, India

ARTICLE INFO

Article history:
Received 27 May 2009
Received in revised form
24 August 2009
Accepted 29 August 2009
Available online 11 September 2009

Keywords:
Nanoparticles
X-ray diffraction
Saturation magnetization
Coercivity
Cation distribution

ABSTRACT

Nanocrystalline manganese substituted lithium ferrites $Li_{0.5}Fe_{2.5-x}Mn_xO_4$ ($2.5 \leq x \geq 0$) were prepared by sol–gel auto-combustion method. X-ray diffraction patterns revealed that as the concentration of manganese increased, the cubic phase changed to tetragonal. Magnetic properties were measured by hysteresis loop tracer technique. All the compositions indicated ferrimagnetic nature. The surface morphology of all the samples was studied by using scanning and transmission electron microscopy. The substitution of manganese ions in the lattice affected the structural as well as magnetic properties of spinels.

1. Introduction

Ferrospinels have interesting structural and magnetic properties and are widely used in many important components such as microwave devices, memory cores, magnetic recording media, transformers, choke coils, high frequency instruments, data storage, noise filters and recording heads, owing to their high magnetic permeabilities and low magnetic losses [1,2]. These properties are dependent on the nature of ions and their charge distribution among tetrahedral and octahedral sites. In spinels, the oxygen ions form a cubic close packed array, in which the A site cations occupy one-eighth of the tetrahedral sites and the B site cations are distributed over one half of the octahedral positions. The modifications of the structural and magnetic properties of ferrites are due to substitution of different ions and have been studied by various workers [3–8].

Here, we report the substitution of manganese in lithium ferrite and its effect on structural and magnetic properties.

2. Experimental details

Polycrystalline samples having the general formula, $Li_{0.5}Fe_{2.5-x}Mn_xO_4$ ($0.0 \leq x \leq 2.5$) were synthesized by sol–gel auto-combustion method. High purity AR grade ferric nitrate, manganese nitrate, lithium nitrate and citric acid were used for synthesis. The metal nitrate solutions were mixed in the required stoichiometric ratios in distilled water. The pH of the solution was maintained between 9 and 9.5 using ammonia solution. The solution mixture was slowly heated around 373 K with constant stirring to a obtain fluppy mass. The precursor powder was sintered at 973 K for 8 hrs then mixed with 2% polyvinyl alcohol as a binder and uniaxially pressed at a pressure of 8 ton/cm^2 to form the pellets.

The phase formation of the samples was confirmed by X-ray diffraction studies using Philips PW-1710 X-ray diffractometer with Cu$K\alpha$ radiation ($\lambda = 1.54056$ Å). The surface morphology and size of sintered powders were studied by scanning electron microscopy (SEM: Model JEOL-JSM6360). A Philips 200 CX transmission electron microscope (TEM) was used to find the particle size by suspending the samples in isopropyl alcohol. The FTIR spectra were recorded using Perkin Elmer FTIR in KBr pellets. Magnetic properties were studied using Hysteresis loop tracer (Magneta B–H loops tracer) at a maximum applied field of 2.5 KOe.

3. Results and discussion

3.1. X-ray diffraction

X-ray diffraction patterns of the Mn-substituted lithium ferrite samples are shown in Fig. 1. From Table 1, it is noted that, the

* Corresponding author.
E-mail addresses: p_hankarep@rediffmail.com (P.P. Hankare), raj_rbm_raj@yahoo.com (R.P. Patil).

0022-4596/$ - see front matter © 2009 Published by Elsevier Inc.
doi:10.1016/j.jssc.2009.08.034

manganese substituted lithium ferrites are cubic in the range $1.5 \leq x \geq 0.0$ and tetragonal in the range of $2.5 \leq x \geq 2.0$. The tetragonal structure for x=2.0 and 2.5 is due to the Jahn–Teller effect of Mn^{3+} ions [9]. The lattice constant increases with substitution of manganese content upto x=1.5, there after decreases due to the tetragonal distortion. The increase in lattice constant with increase in Mn content is due to the higher ionic radii of Mn^{3+} (0.645 Å) ions as compared to Fe^{3+} (0.64 Å) ions. (Table 1). From the X-ray diffraction peaks, average particle size was estimated using Scherrer's formula.

$$t = 0.9\lambda/\beta \operatorname{Cos}\theta \quad (1)$$

where, symbols have their usual meaning.

The X-ray density (dx) was calculated using the following relation.

$$dx = 8M/Na^3 \quad (2)$$

where, N is the Avagadros number (6.023×10^{23} atom/mol), M is Molecular weight and a is Lattice constant.

The values of lattice constant (a), crystallite size (t) and X-ray density (dx) are summarized in Table 1.

The cation distribution for all the compositions were determined from X-ray diffraction intensity calculations using the method suggested by Burger [10]. The X-ray intensity calculations were carried out using the following formula [11].

$$I_{hkl} = |F_{hkl}|^2 P_m L_p \quad (3)$$

where, I_{hkl} is the relative integrated intensity, F_{hkl} the structural factor, P_m the multiplicity factor and L_p is the Lorentz polarization factor,

$$L_p = 1 + \operatorname{Cos}^2 2\theta / \operatorname{Sin}^2 \theta \operatorname{Cos}\theta \quad (4)$$

According to Ohnishi and Teranishi [12] the intensity ratios of the planes I_{220}/I_{400} and I_{220}/I_{440} are considered to be sensitive to the cation distribution. Miller [13] has calculated the octahedral site preference energies of various transition metal ions using the concept of crystal field stabilization energy. According to him Fe^{3+} has strong preference for tetrahedral co-ordination as compared to Li^+ and Mn^{3+} ions. ($Fe^{3+} \rightarrow 13.3$, $Li^+ \rightarrow 3.6$ and $Mn^{3+} \rightarrow -3.1$ Kcal/g.at.wt).

To determine cation distribution and its variation with composition, the intensity ratios (I_{220}/I_{400}, I_{220}/I_{440}) for different compositions were calculated and then were compared with the observed intensity ratios (Table 2). From X-ray intensity calculations, it is observed that as the concentration of Mn^{3+} increases in the lattice they prefer to occupy octahedral site while Fe^{3+} ions prefer tetrahedral coordination. This is in good agreement with the site preferences calculated by Miller [13].

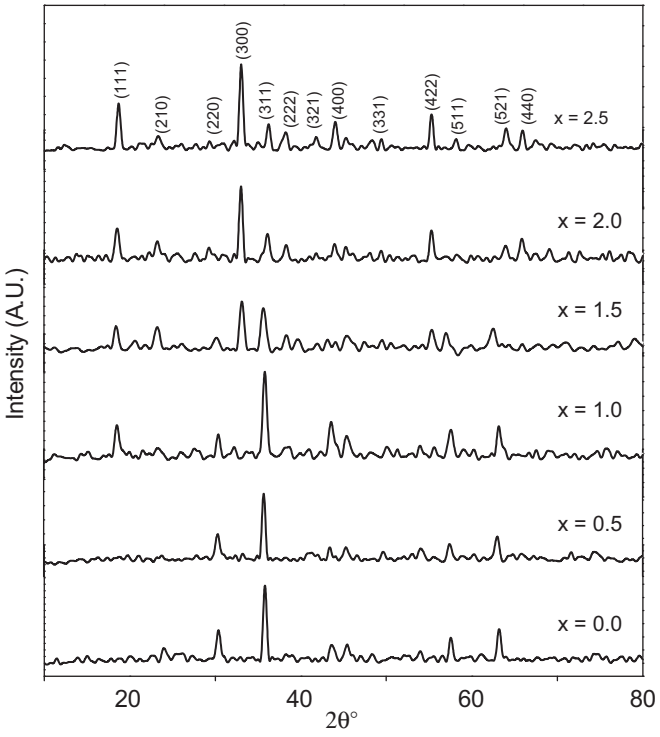

Fig. 1. X-ray diffraction patterns of $Li_{0.5}Fe_{2.5-x}Mn_xO_4$ system, (x=0.0, 0.5, 1.0, 1.5, 2.0 and 2.5).

Table 1
Lattice constant, crystallite size and X-ray density for $Li_{0.5}Fe_{2.5-x}Mn_xO_4$ system.

Composition x	Lattice constant (a) (Å)	Crystallite size (t) (nm)	X-ray density (dx) (gm/cm^3)
0.0	8.30	29	4.8
0.5	8.32	32	4.7
1.0	8.33	32	4.7
1.5	8.39	32	4.6
2.0	$a=b$=5.6724, c=8.747	33	4.9
2.5	$a=b$=5.4194, c=9.666	33	5.0

3.2. Infra-red study

The FTIR absorption spectra were recorded in the range 350–1000 cm^{-1}. The IR spectra for Mn substituted lithium ferrospinels show two strong bands. The high frequency band v_1 is in the range 586–610 cm^{-1}and the lower frequency band v_2 is in the range 440–466 cm^{-1}. The high frequency band is due to the

Table 2
Cation distribution for $Li_{0.5}Fe_{2.5-x}Mn_xO_4$ system.

Composition x	Cation A sites	Cation B sites	Intensity ratio I_{220}/I_{400}		Intensity ratio I_{220}/I_{440}	
			Expt.	Calc.	Expt.	Calc.
0.0	$Fe_{[1.0]}$	$Fe_{[1.5]}$ $Li_{[0.5]}$	2.2972	2.3465	1.011	1.020
0.5	$Fe_{[0.95]}$ $Li_{[0.05]}$	$Fe_{[1.05]}$ $Mn_{[0.5]}$ $Li_{[0.45]}$	1.9429	1.955	0.9455	0.9565
1.0	$Fe_{[0.90]}$ $Li_{[0.1]}$	$Fe_{[0.6]}$ $Mn_{[1.0]}$ $Li_{[0.40]}$	1.1100	1.103	1.05	1.04
1.5	$Fe_{[0.85]}$ $Li_{[0.15]}$	$Fe_{[0.15]}$ $Mn_{[1.5]}$ $Li_{[0.35]}$	1.2097	1.3021	1.1012	1.0819
2.0	$Mn_{[0.3]}$ $Fe_{[0.5]}$ $Li_{[0.2]}$	$Mn_{[1.7]}$ $Li_{[0.3]}$	0.7084	0.7230	1.760	1.793
2.5	$Mn_{[0.75]}$ $Li_{[0.25]}$	$Mn_{[1.75]}$ $Li_{[0.25]}$	0.60	0.583	1.813	1.803

vibration of the tetrahedral M–O bond and the low frequency band is due to the vibration of the octahedral M–O bond. The force constant was calculated for tetrahedral site (k_t) and octahedral site (k_o) using method suggested by Waldron [14].

$$k_t = 7.62 \times M_1 \times \upsilon_1^2 \times 10^{-7}\ \mathrm{N/m} \quad (5)$$

$$k_o = 10.62 \times M_2/2 \times \upsilon_2^2 \times 10^{-7}\ \mathrm{N/m} \quad (6)$$

where, M_1 and M_2 are the molecular weights of cations at A and B sites, respectively. The variation of the force constant with Mn content is represented in Table 3. The force constant increases with Mn and reveals the strengthening of interatomic bonding.

3.3. Scanning electron microscopy

The SEM images of Mn substituted lithium ferrites are shown in the Fig. 2(a–c). It is observed that, the average grain size goes on increasing on substitution of Mn content. The average grain size was smaller than 0.1 μm for all compositions.

Table 3
IR frequency and force constants for $Li_{0.5}Fe_{2.5-x}Mn_xO_4$.

Composition x	$\upsilon_1\ \mathrm{cm}^{-1}$	$\upsilon_2\ \mathrm{cm}^{-1}$	$k_t \times 10^2$ N/m	$k_o \times 10^2$ N/m
0.0	586	466	1.463	1.009
0.5	594	455	1.501	0.9548
1.0	607	449	1.567	0.9258
1.5	607	447	1.570	0.9130
2.0	608	445	1.560	0.9050
2.5	610	440	1.550	0.8831

3.4. Transmission electron microscopy

The morphology and grain size of manganese substituted lithium ferrites powders were characterized by TEM (Fig. 3a). In lithium ferrite, it is noted that all particles are uniform and the average grain size is ~50 nm. Selected area electron diffraction pattern (SAED) of the particles is shown in the Fig. 3b. It suggests the polycrystallinity of individual crystallite and also confirms the formation of spinel ferrites.

3.5. Magnetic measurements

The hysteresis studies of $Li_{0.5}Fe_{2.5-x}Mn_xO_4$ system, was carried out using a magenta B–H loop tracer. The hysteresis loops are shown in Fig. 4(a–c). The ferrimagnetic behavior was shown by all the samples. The decreasing trend in saturation magnetization (Ms) and increasing values of coercivity (Hc) is observed with substitution of Mn ions (Table 4). The decreasing trend in saturation magnetization with increasing concentration of manganese is due to the A–O–B interactions in ferrites [15] and also the stronger covalency effect arising due to various cationic site dimensions.

The experimental magnetic moment is calculated by the following relation [16].

$$n_\beta = \mathrm{MW} \times \mathrm{Ms}/5585 \quad (7)$$

where, MW is the molecular weight of composition (in grams), Ms is saturation magnetization (in Oe) and 5585 is magnetic factor.

According to the Neel's theory, the calculated magnetic moment per formula unit in (μ_β), n_β^N is expressed using following equation; [17]

$$n_\beta^N = M_B(X) - M_A(X) \quad (8)$$

From Table 4, it is noted that magnetic moment observed from hysteresis measurements goes on decreases with increase in Mn content. The μ_β calculated from the cation distribution (Table 2)

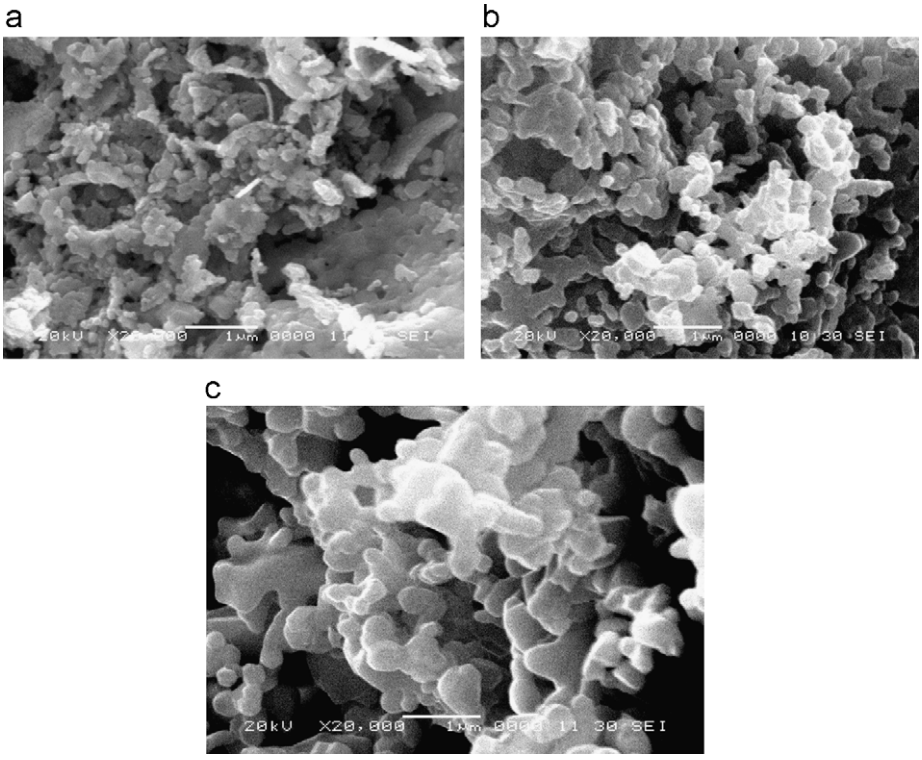

Fig. 2. SEM images for $Li_{0.5}Fe_{2.5-x}Mn_xO_4$, (a) x=0.0, (b) x=1.0 and (c) x=2.0.

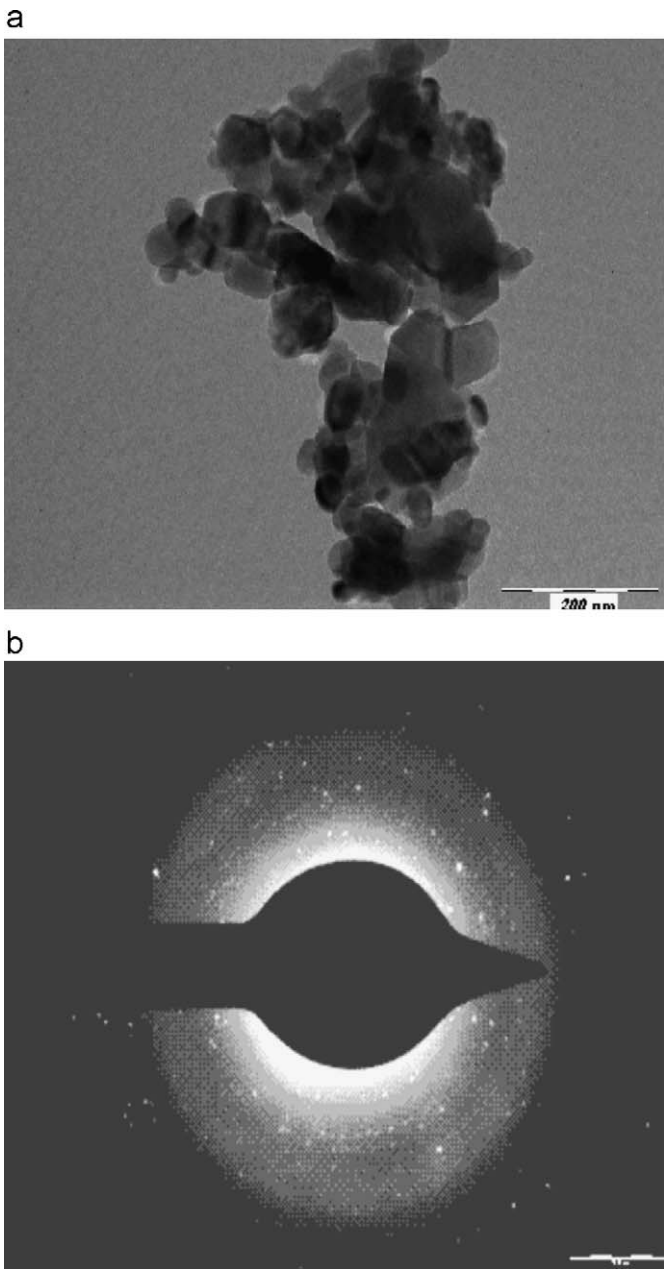

Fig. 3. (a) TEM image for $Li_{0.5}Fe_{2.5}O_4$. (b) SAED pattern for the compound $Li_{0.5}Fe_{2.5}O_4$.

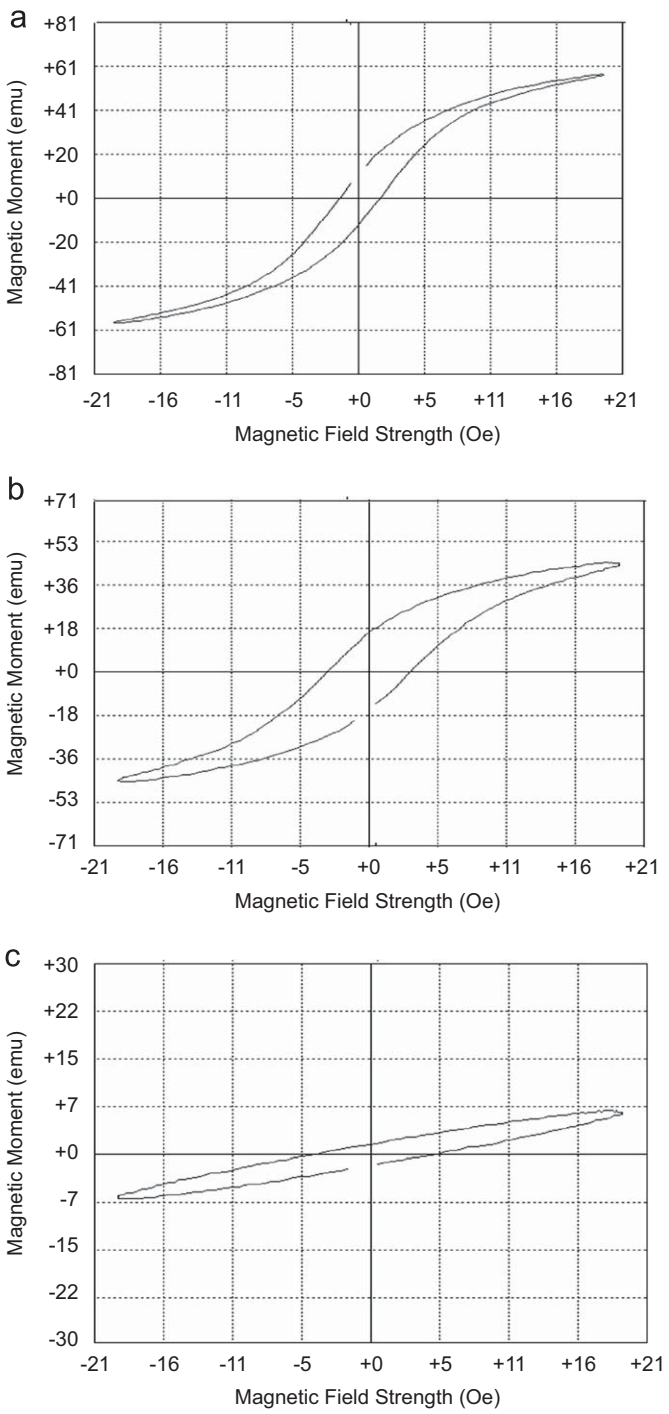

Fig. 4. Hysteresis loops of $Li_{0.5}Fe_{2.5-x}Mn_xO_4$ system, (a) $x=0.0$, (b) $x=1.0$ and (c) $x=2.5$.

obtained from X-ray intensity calculations is given in Table 4. From Table 4, it is noted that observed and calculated magnetic moments show variation. This cannot be explained on the basis of Neel's model. This behavior can only be explained on the basis of Yafet–Kittel [18] triangular magnetic ordering on B site ions leading to the reduction in A–O–B interactions. The large variation in calculated and observed magnetic moment with increase in Mn content can be correlated to the increasing values of Y–K angles (Table 4).

4. Conclusions

Manganese substituted lithium ferrites of nanocrystalline nature were synthesized by sol–gel auto-combustion method. The distribution of cations in $Li_{0.5}Fe_{2.5-x}Mn_xO_4$ system has been studied using Burger method. The system shows cubic phase for $x \leq 1.5$ and tetragonal for $x \geq 2.0$. From X-ray intensity calculations, it is noted that Mn^{3+} ions show strong preference towards octahedral site. The ferrospinels synthesized by auto-combustion method were in nanocrystalline range ($\sim$50 nm). The saturation magnetization and coercivity showed decreasing trend with increase in Mn content. The calculated and observed values of magnetic moment indicated large variation which is due to canting of spins at octahedral site.

Table 4
Saturation magnetization, magnetic moment and Y–K angles for the system $Li_{0.5}Fe_{2.5-x}Mn_xO_4$.

Composition x	Saturation magnetization (emu/g)	Magnetic moment (μ_β) Observed	Magnetic moment (μ_β) Calculated	Y–K angles α^0_{YK}
0.0	57.41	2.1287	2.5	18
0.5	41.43	1.532	2.5	29
1.0	45.04	1.662	2.5	28
1.5	18.56	0.6836	2.5	43
2.0	14.43	0.5303	2.7	48
2.5	6.85	0.2512	4.0	62

Acknowledgment

Author (PPH) is very thankful to UGC, New Delhi for financial assistance through Major research project F.No.32–289/2006 (SR).

References

[1] G. Blasse, Philips Res. Rep. (Netherlands) 20 (1965) 528.
[2] J.B. Goodenough, Magnetism and Chemical Bond, Wiley, New York, 1966.
[3] J.B. Goodenough, A.L. Loeb, Phys. Rev. 98 (1955) 391.
[4] A.P.B. Sinha, N.R. Sanjana, A.B. Biswas, Acta Cryst. 10 (1957) 439.
[5] P. Nathawani, V.S. Darshane, J. Phys. C (Solid State Phys.) 2 (1988) 3191.
[6] G.R. Dube, V.S. Darshane, Bull. Chem. Soc. Japan 64 (1991) 2449.
[7] S.C. Watawe, U.A. Bamne, S.P. Gonbare, R.B. Tangsali, Mater. Chem. Phys. 103 (2007) 323.
[8] S. Singhal, S.K. Barthwal, K. Chandra, Indian J. Pure Appl. Phys. 45 (2007) 821.
[9] M.M. Thackeray, W.I.F. David, D.G. Bruce, J.B. Goodenough, Mater. Res. Bull. 18 (1983) 461.
[10] M.J. Buerger, Crystal Structure Analysis, Wiley, New York, 1960, p. 46.
[11] B.D. Cullity, Elements of X-ray Diffraction, Addison-Wesley Publishing, Reading, MA, 1956 352.
[12] H. Ohinishi, T. Teranishi, J. Phys. Soc. Jpn. 6 (1969) 36.
[13] A. Miller, J. Appl. Phys. 30 (1959) 245.
[14] R.D. Waldron, Phys. Rev. 99 (1955) 1727.
[15] Y.-P. Fu, C.-S. Hsu, Solid State Commun. 134 (2005) 201.
[16] Jan Smit, Magnetic Properties of Materials, Intra-University Electronics Series, vol. 13, 1971, p. 89.
[17] L. Neel, C.R. Acad. Sci. 230 (1950) 375.
[18] Y. Yafet, C. Kittel, Phys. Rev. 90 (1992) 29.